Chinese Journal of Integrative Medicine
Available online at link.springer.com/journal/11655
Journal homepage: www.cjim.cn/zxyjhen/zxyjhen/ch/index.aspx
E-mail: cjim_en@cjim.cn

Original Article

Effect of Shengmai Yin on Epithelial-Mesenchymal Transition of Nasopharyngeal Carcinoma Radioresistant Cells*

WANG Ze-tai[1], PENG Yan[1], LOU Dan-dan[1], ZENG Si-ying[1], ZHU Yuan-chao[1], LI Ai-wu[2], LYU Ying[2], ZHU Dao-qi[1], and FAN Qin[1]

ABSTRACT **Objective:** To investigate the mechanism by which Chinese medicine Shengmai Yin (SMY) reverses epithelial-mesenchymal transition (EMT) through lipocalin-2 (LCN2) in nasopharyngeal carcinoma (NPC) cells CNE-2R. **Methods:** Morphological changes in EMT in CNE-2R cells were observed under a microscope, and the expressions of EMT markers were detected using quantitative real-time PCR (RT-qPCR) and Western blot assays. Through the Gene Expression Omnibus dataset and text mining, LCN2 was found to be highly related to radiation resistance and EMT in NPC. The expressions of LCN2 and EMT markers following SMY treatment (50 and 100 μg/mL) were detected by RT-qPCR and Western blot assays *in vitro*. Cell proliferation, migration, and invasion abilities were measured using colony formation, wound healing, and transwell invasion assays, respectively. The inhibitory effect of SMY *in vivo* was determined by observing a zebrafish xenograft model with a fluorescent label. **Results:** The CNE-2R cells showed EMT transition and high expression of LCN2, and the use of SMY (5, 10 and 20 μg/mL) reduced the expression of LCN2 and reversed the EMT in the CNE-2R cells. Compared to that of the CNE-2R group, the proliferation, migration, and invasion abilities of SMY high-concentration group were weakened ($P<0.05$). Moreover, SMY mediated tumor growth and metastasis in a dose-dependent manner in a zebrafish xenograft model, which was consistent with the *in vitro* results. **Conclusions:** SMY can reverse the EMT process of CNE-2R cells, which may be related to its inhibition of LCN2 expression. Therefore, LCN2 may be a potential diagnostic marker and therapeutic target in patients with NPC.

KEYWORDS epithelial-mesenchymal transition, lipocalin-2, nasopharyngeal carcinoma, radiation therapy, Shengmai Yin, Chinese medicine

Nasopharyngeal carcinoma (NPC) is a malignant tumor of the head and neck that originates from the epithelium. The incidence rate of NPC is high,[1] and intensity modulated radiation therapy (IMRT) is the primary treatment for NPC.[2] However, NPC cells can repair radiation-induced damage in various ways, resulting in radiation resistance. After acquiring radiation resistance, NPC cells are prone to recurrence and distant metastasis, and distant metastasis is closely related to epithelial-mesenchymal transition (EMT).[3] EMT is a process in which quiescent epithelial cells are transformed into mobile mesenchymal cells.[4] It is well known that cancer cells promote migration and invasion through EMT, thus ensuring their survival and malignancy. Increasing evidence has shown that EMT leads to tumor radiotherapy resistance, and it is related to the low survival rate of cancer patients.[5,6] Previous study has shown that the special AT-rich sequence binding protein 1 (SATB1) leads to radiation and drug resistance in NPC by promoting EMT and enhancing matrix metalloproteinase (MMP)-9 expression.[5] Other studies have shown that interleukin (IL)-6 can regulate the EMT process and radiation resistance in NPC cells.[3] These studies on EMT and radiation resistance suggest that tumors may be resistant to radiotherapy via the EMT pathway. However, the role of EMT in radiation resistance of NPC cells remains unclear.

Lipocalin-2 (LCN2), also known as neutrophil

*Supported by the National Natural Science Foundation of China (No. 82074132), Project of Administration of Traditional Chinese Medicine of Guangdong Province of China (No. 20213009) and the Science and Technology Plan Project of Guangzhou City (No. 202102080405)

1. School of Traditional Chinese Medicine, Southern Medical University, Guangzhou (510515), China; 2. Department of Traditional Chinese Medicine, Nanfang Hospital (510515), China
Correspondence to: Prof. FAN Qin, E-mail: fqin@163.com

DOI: https://doi.org/10.1007/s11655-022-3689-2

gelatinase-associated lipid carrier protein (NGAL), belongs to the lipid carrier protein superfamily and is a secretory glycoprotein of the adipofactor superfamily.[7] An increasing number of studies have confirmed that LCN2 is very important for various tumor-related processes. High levels of LCN2 are associated with increased cell proliferation, angiogenesis, invasion, and metastasis.[8] A previous study showed that the EMT process can be reversed by inhibiting the LCN2 and LCN2/Twist1 signaling pathway, thereby inhibiting nasal mucosal remodeling in mice with chronic sinusitis.[9] These findings suggest that LCN2 plays an important role in EMT in several tumors. However, the effect of LCN2 on the EMT process in NPC radiation resistance remains unclear.

Chinese medicine has certain advantages in the adjuvant treatment of tumor diseases. Shengmai Yin (生脉饮, SMY), a classic formula in Chinese medicine, is composed of *Radix ginseng*, *Ophiopogon japonicus* and *Schisandra chinensis*. It is a famous prescription for tonifying qi and yin. SMY has been used to treat chest stuffiness,[10] palpitation[11] and other diseases.[12] Modern pharmacological studies have shown that SMY has received more and more attention for its adjunctive therapeutic effect in radiotherapy and chemotherapy of tumors.[13,14] Our previous study have shown that SMY, (50 μg/mL, 48 h) affects radiosensitization.[15] In the current study, the potential of LCN2 was evaluated as a biomarker of NPC EMT by analyzing the Gene Expression Omnibus (GEO) dataset (GSE48501) and text mining. In addition, the relationship between LCN2 and NPC proliferation, migration, and invasion as well as the therapeutic effects of SMY was studied.

METHODS

Cell Culture

The human NPC cell line, CNE-2, was obtained from the Cancer Center of Sun Yat-sen University (Guangzhou, China). The CNE-2 cells were induced by long-term high-dose radiation to obtain a stable radioresistant cell line, CNE-2R.[16] The cells were cultured in RPMI-1640 medium (Gibco, USA) containing 10% fetal bovine serum (FBS, Gibco) at 37 ℃ and 5% CO_2.

Reverse Transcription-Quantitative Polymerase Chain Reaction

The total RNA was extracted using the TRIzol reagent. Complementary DNA (cDNA) was synthesized from the RNA template using a cDNA synthesis kit (Takara Biotechnology, China). The experiment was performed using the SYBR Green reaction mixture (Bimake, USA). The reverse transcription reaction conditions were as follows: 37 ℃ for 15 min, 85 ℃ for 5 s, and 4 ℃ for an unlimited time. The polymerase chain reaction (PCR) amplification conditions were as follows: first, 95 ℃ for 10 min; 40 cycles of 15 s at 95 ℃, 30 s at 60 ℃, and 30 s at 72 ℃; and 95 ℃ for 15 s, 60 ℃ for 60 s, and 95 ℃ for 15 s. The PCR reaction was performed on a Roche Light Cycler 96 (Switzerland), and the mRNA expression fold was calculated by the Ct ($2^{-\triangle\triangle CT}$) method. The primers used in real time are shown in Table 1.

Table 1. Primers Used in Real-Time PCR Reaction

Primer	Sequence	Size
LCN2	5'-GCTGACTTCGGAACTAAAGGAGAA-3'	24
	5'-GGGAAGACGATGTGGTTTTCA-3'	21
Snail	5'-ACATCCGAAGCCACACG-3'	17
	5'-TGGGGACAGGAGAAGGG-3'	17
CDH-1	5'-CGAGAGCTACACGTTCACGG-3'	20
	5'-GGCCTTTTGACTGTAATCACACC-3'	23
GAPDH	5'-ATCATCAGCAATGCCTCCTG-3'	20
	5'-ATGGACTGTGGTCATGAGTC-3'	20

Western Blot Assay

The CNE-2 cells was used as the control. CNE-2R cells were divided into 3 groups: CNE-2R, CNE-2R+SMY (50 μg/mL), and CNE-2R+SMY (100 μg/mL). The CNE-2R cells were cultured at a suitable density and treated with 0, 50, or 100 μg/mL SMY (2004091, Lei Yunshang, China) for 48 h. The collected cells were lysed in radio immunoprecipitation assaylysis (RIPA) buffer containing a protease and phosphatase inhibitor mixture (Sigma-Aldrich Corp, USA). Then, the cell lysates were separated by sodium dodecyl sulfate-polyacrylamide gel electrophoresis (SDS-PAGE) and transferred to polyvinylidene fluoride membranes. The membrane strips were immersed in a primary antibody solution (Affinity, China) and incubated with secondary antibodies (Abbkine, China). Primary antibodies were diluted in a ratio of 1:1000 and secondary antibodies 1:5000. Finally, an enhanced chemiluminescence kit (Millipore, USA) was used for detection.

Text Mining and Microarray Data Analysis

Text-mining approach was used to search for genes related to EMT in the website Genclip3 (http://

cismu.net/genclip3/analysis.php). When a keyword was provided by the user, gene symbols found in published PubMed articles related to keywords can be retrieved and extracted. When the keyword "EMT or Epithelial mesenchymal transition" was input into Geneclip3, all the displayed genes make up the text mining genes (Text Mining). Then, GSE48501 dataset was downloaded from NCBI Gene Expression Omnibus (GEO) website. The dataset included 2 radioresistant NPC samples and 2 radiosensitive NPC samples in total. Differential gene analysis was conducted through geo2R tool. $|\text{Log FC}| \geqslant 2$ and $P<0.05$ were used as screening conditions to obtain differential expression genes (DEGs). The intersection of Text Mining and DEGs were overlapping genes, and then were kept for further analysis.

Cell Counting Kit-8 Assay

The cells were taken in the logarithmic growth phase, and the cell concentration was adjusted to 2×10^4 cells/mL with complete culture medium containing 10% FBS. Each well of a 96-well culture plate was seeded with 100 μL. Cells were treated with SMY at 0, 12.5, 25, 50, 100, 200, 400, and 800 μg/mL, with 5 replicate wells for each group. After incubation at 37 ℃ for 48 h, the culture was terminated and 10 μL of cell counting kit-8 (CCK-8) solution (Abbkine) was added to each well. After incubation at 37 ℃ for 2 h, the optical density (OD) of each well were obtained at 450 nm to calculate the cell proliferation activity: cell proliferation activity (%) = $(OD_{plus\ drug}–OD_{blank})/(OD_{control}–OD_{blank})\times100\%$.

Colony Formation Assay

The cells were seeded in a 6-well plate at the same cell density. Then, the cells were incubated at 37 ℃ for 24 h for attachment and treated with 0, 50, and 100 μg/mL SMY for 48 h. The cells were cultured for 14 day to form colonies. The cells were then fixed with 4% paraformaldehyde and stained with 0.1% crystal violet solution. Colonies containing at least 50 cells were included, and the following formula was used: colony formation rate (%) = (number of clones/number of inoculated cells) × 100%.

Wound Healing Assay

A wound healing assay was used to determine the effect of SMY on the cell migration capability. Each group of cells was treated with SMY at concentrations of 0, 50 and 100 μg/mL and incubated at 37 ℃ for 48 h. Then, cells (approximately 1×10^6 cells/well) were seeded in 6-well plates and routinely cultured at 37 ℃ and 5% CO_2 overnight. Cultured cells were grown to 80% confluence, and 3 perpendicular lines were scratched in each well using a yellow (200 μL) sterile pipette tip. The growth medium was then removed, and the cells were gently washed 3 times with phosphate-buffered saline (PBS). After the PBS was aspirated, the cells were cultured in serum-free media. Images were taken at 0 and 24 h. The percentage of migration was calculated using the ImageJ software (NIH, USA). The percentage of wound healing was calculated using the following formula: 100%–(area after 24 h/area at 0 h) × 100%.

Transwell Invasion Assay

The transwell chamber (Corning, USA) with matrigel (BD, China) was used to detect cell invasion. The cells were first treated with 0, 50 and 100 μg/mL SMY for 48 h. Then, each group of cells was seeded into each upper chamber with 200 μL of serum-free medium at a density of 2×10^5 cells/mL, and 800 μL of medium containing 10% FBS was added to each lower chamber. After incubation for 24 h, the cells on the upper surface were completely removed. Cells were fixed with 4% paraformaldehyde for 20 min, and then stained with 0.5% crystal violet for 20 min. Three replicate holes were placed in each group. The number of cells was counted with an inverted microscope (Ti-S1, Nikon, Japan) under a high-power lens (200×) in a random field of view.

Microinjection of Zebrafish

The zebrafish wild-type AB strain (Danio rerio) was purchased from the National Zebrafish Resource Center, Hubei, China. Adult zebrafish were maintained under standard laboratory conditions and embryos were produced by natural mating (2:2).[17] Embryos 2 day post-fertilization (2 dpf) were anesthetized with tricaine (Sigma Aldrich Corp), placed on a Petri dish for microinjection, and treated with SMY (0, 5, 10 and 20 μg/mL, 48 h) at 3 day post-fertilization (3 dpf). After 48 h, the drug effect was observed at 5 day post-fertilization (5 dpf).[18] All experiments using zebrafish were in accordance with the ethical approval of the Institutional Animal Care and Use Committee of Southern Medical University, China.

Statistical Analysis

All experiments were repeated independently at least 3 times. SPSS software (version 21.0, IBM, USA) was used for the statistical analysis. All data

Chin J Integr Med 2023 Aug;29(8):691-698

were provided in the form of mean ± standard deviation ($\bar{x} \pm s$). One-way analysis of variance (ANOVA) followed by Student's *t*-test were used for for statistical comparison. Statistical significance was set at *P*-value less than 0.05.

RESULTS

EMT Appeared in CNE-2R Cells

The CNE-2R cells exhibited typical morphological changes during EMT (Figure 1A). The reverse transcription-quantitative PCR (RT-qPCR) results showed that in the CNE-2R cells, the expression of snail and vimentin significantly increased (P<0.01, Figure 1B). In addition, Western blot analysis showed that the expression of E-cadherin was reduced in the CNE-2R cells compared to that in the CNE-2 cells, whereas the expression of E-cadherin and vimentin was increased (P<0.05 or 0.01, Figures 1C and 1D).

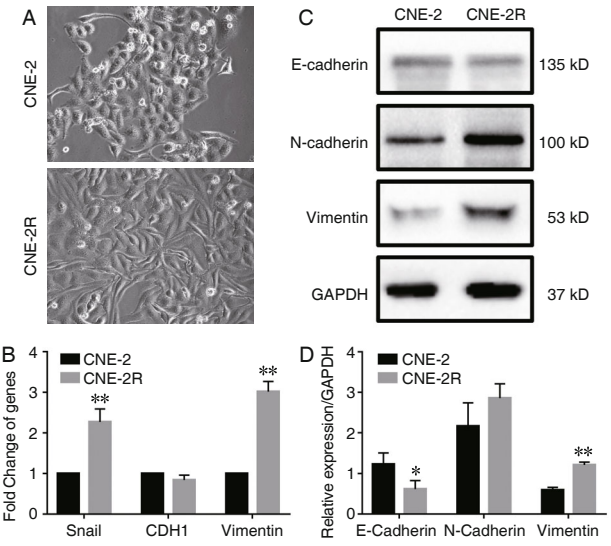

Figure 1. CNE-2R Cells Had EMT Phenotype

Notes: (A) CNE-2R cells produced spindle shape changes under microscope. (B) Expressions of EMT-related genes in the CNE-2R cells were verified by reverse transcription-quantitative PCR assay. (C, D) Expressions of EMT-related proteins in the CNE-2R cells were verified by Western blot assay. Epithelial-mesenchymal transition; $^{*}P$<0.05, $^{**}P$<0.01 *vs*. CNE-2 cell group

Screening of Target Genes

Based on the text mining and microarray data analysis, it was concluded that there were 375 genes related to EMT in Geneclip3, and 400 differentially expressed genes in the radioresistance-related chip GSE48501 for NPC. There were 23 intersection genes, which are molecules related to EMT and radioresistance (Figures 2A–2C, Table 2). Among the upregulated genes, LCN2 had the largest difference multiple, and the logFC was 2.74. The highly expressed genes were focused on, and then RT-qPCR was used to verify the top 5 highly expressed genes. The results showed

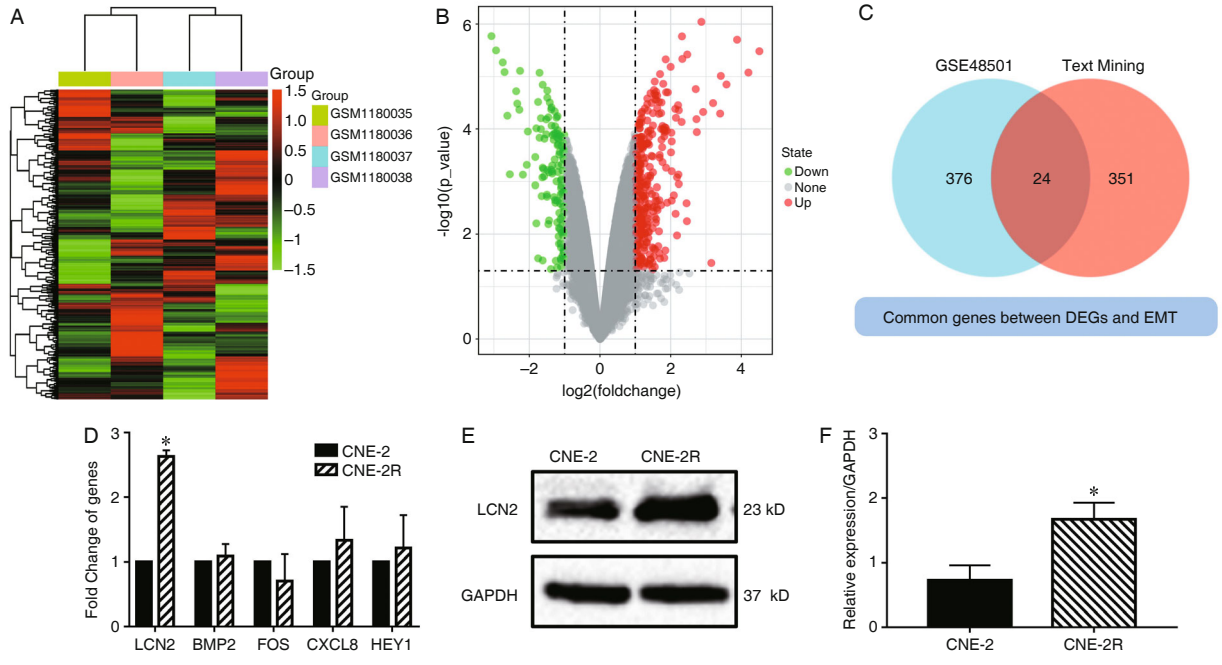

Figure 2. Screening of Differential Genes

Notes: (A, B) The heat map and volcano map related to different genes of radiation resistance were obtained through the analysis of the GSE48501 chip. (C) Through the gene difference analysis and text mining intersection, the intersection genes were defined as 24 genes related to radiation resistance and epithelial–mesenchymal transition. (D) The top 5 highly expressed genes were verified by quantitative real-time PCR assay, $^{*}P$<0.01 *vs*. CNE-2. (E, F) The expressions of lipocalin-2 (LCN2) in the cells were detected by Western blot assay, $^{*}P$<0.01 *vs*. CNE-2

Table 2. Epithelial-Mesenchymal Transition- and Radiation Resistance-Associated Candidate Genes

Gene symbol	Log2FC	*P*-value
LCN2	2.74	1.15E-04
BMP2	2.45	2.58E-03
FOS	2.13	4.16E-05
CXCL8	1.82	1.97E-01
HEY1	1.81	1.03E-04
VEGFA	1.73	2.81E-03
NUPR1	1.72	8.44E-02
IFI27	1.56	1.95E-02
S100A9	1.41	8.51E-04
S100A8	1.39	2.64E-03
IL6	1.38	3.85E-02
HOTAIR	1.26	2.05E-02
MUC1	1.06	3.43E-04
SMAD6	1.06	3.58E-03
TRIM2	1.05	4.14E-03
SCNN1A	1.04	1.51E-04
KRT14	–2.75	5.40E-06
GJA1	–1.83	1.18E-03
THBS1	–1.67	1.01E-04
KRT6A	–1.46	6.00E-05
SERPINB3	–1.21	5.98E-03
SMY SIX2	–1.15	3.94E-03
CCDC88C	–1.07	1.68E-03

that the expression of LCN2 in the CNE-2R cells was 2.634 ± 0.076 folds of that in the CNE-2 group (*P*<0.01). There was no significant difference in the expression of other genes (*P*>0.05, Figure 2D). Western blot assay results showed that the expression of LCN2 protein in the CNE-2R cells was 2.393 ± 0.431 folds higher than that in the CNE-2 group (*P*<0.01, Figures 2E and 2F).

SMY Reverses EMT through LCN2 in CNE-2R Cells

After 48 h of administration, the inhibitory effect of SMY on the CNE-2R cells increased significantly with increasing concentration in a dose-dependent manner. Among them, the half-maximal inhibitory concentration (IC_{50}) was 159.11 μg/mL. In the following experiment, two concentrations (50 and 100 μg/mL) without obvious growth inhibition of CNE-2R cells were selected as low and high concentrations, respectively, for 48 h (Figure 3A). The results of the RT-qPCR showed that compared with that of the CNE-2R group, the snail, vimentin, and LCN2 genes in the high-concentration group were significantly downregulated (*P*<0.05, Figure 3B), while the expression of the CDH-1 gene increased (*P*<0.01). Western blot assay results showed that compared with that of the CNE-2R cells, the high-concentration group had relatively low levels of N-cadherin, vimentin, and LCN2 protein expressions (*P*<0.05), and higher expression of E-cadherin (*P*<0.05, Figures 3C and 3D).

SMY Inhibits Proliferation, Migration, and Invasion of CNE-2R Cells

In the colony formation assay, the CNE-2R cells formed more colonies than that of the CNE-2 cells (*P*<0.01). In contrast, the colony formation rate in the CNE-2R cells after treatment with high concentrations of SMY decreased significantly (*P*<0.01, Figures 4A and 4B). In the wound healing assay, compared with that in the CNE-2 group, the cell migration rate in the CNE-2R group increased (*P*<0.01). The cell migration rate decreased significantly in the high-concentration group of SMY (*P*<0.01, Figures 4C and 4D). The results of the transwell invasion assay showed that SMY significantly reduced the number of invasive cells compared to that of the CNE-2R group (*P*<0.01, Figures 4E and 4F).

SMY Inhibits Proliferation and Migration of CNE-2R Cells in Zebrafish

The effects of SMY on tumor proliferation

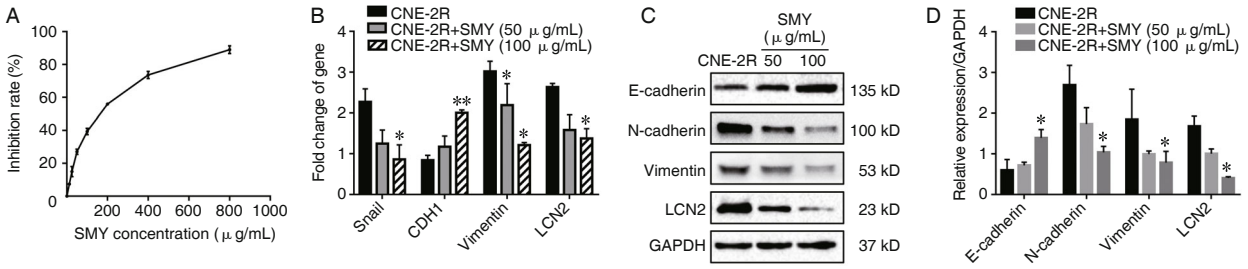

Figure 3. SMY Inhibits EMT Process of CNE-2R Cells *in vitro*

Notes: (A) Concentration of SMY in the CNE-2R cells was detected by the CCK-8 assay. Expression of EMT-related genes in the CNE-2R cells after SMY treatment was detected by reverse transcription-quantitative PCR (B) and Western blot assay (C, D). SMY: Shengmai Yin; EMT: epithelial-mesenchymal transition; **P*<0.05, ***P*<0.01 *vs*. CNE-2R

Chin J Integr Med 2023 Aug;29(8):691-698

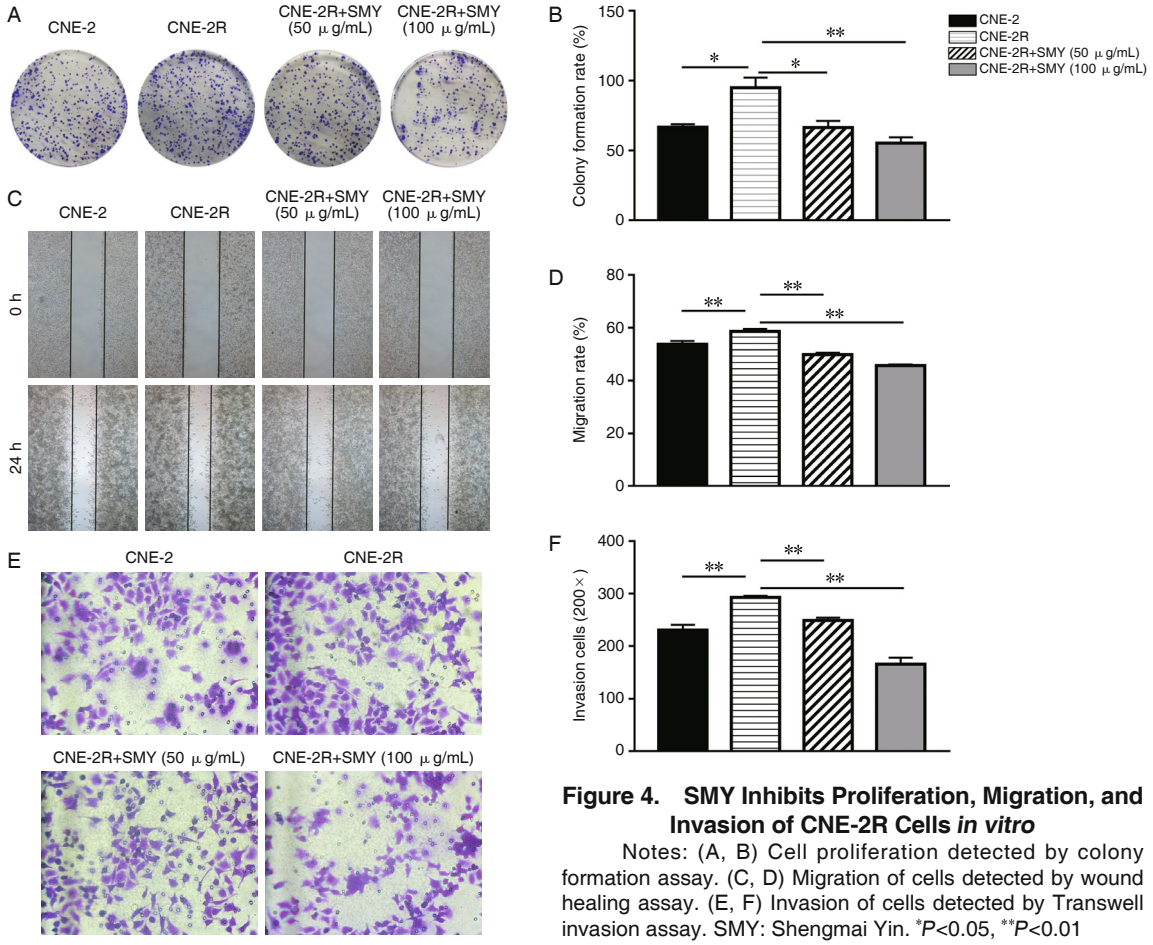

Figure 4. SMY Inhibits Proliferation, Migration, and Invasion of CNE-2R Cells *in vitro*

Notes: (A, B) Cell proliferation detected by colony formation assay. (C, D) Migration of cells detected by wound healing assay. (E, F) Invasion of cells detected by Transwell invasion assay. SMY: Shengmai Yin. $^{*}P<0.05$, $^{**}P<0.01$

and migration *in vivo* were evaluated in a zebrafish xenograft model by implanting CNE-2 and CNE-2R cells with fluorescent labels. After 48 h of drug treatment, the survival rate of zebrafish was calculated, and the median lethal dose of SMY in the transplanted tumor model in the CNE-2R group was 28.64 μg/mL (Figure 5A). In comparison to the fluorescence intensity of the CNE-2 group, that of the CNE-2R group was higher, while that of the SMY group decreased, which was positively correlated with the increase in the SMY concentration (Figures 5B and 5C). By calculating the fluorescence intensity, it was observed that the inhibition rates increased with increasing concentration of SMY (Figure 5D). Additionally, with an increase in SMY concentration, the number of zebrafish with tumor metastasis decreased ($P<0.05$, Figures 5E and 5F).

DISCUSSION

The prevalence of NPC is very high in East and Southeast Asia.[19] This disease is mostly characterized as poorly differentiated squamous cell carcinoma and is highly sensitive to radiotherapy. Therefore, radiotherapy has always been the primary treatment for NPC.[20] However, due to inherent or acquired radioresistance, patients still experience distant metastasis and tumor recurrence during treatment.[21] Overcoming this obstacle has become an urgent challenge in clinical treatment. Therefore, this study aimed to explore the mechanism of radioresistance in NPC and provide new targets and drugs for reversing radioresistance in NPC.

In the present study, NPC cells were treated with radiation. It was found that the morphological changes of the CNE-2R cells and the EMT-related marker E-cadherin were downregulated, while N-cadherin and vimentin were upregulated, suggesting that the radiation resistance of cancer cells may be related to EMT. Recent study has pointed out that EMT is a basic process involved in radiation resistance, and its mechanism may be related to the EMT-related signaling pathway, EMT-inducing transcription factors, and EMT-related non-coding RNAs.[22]

In order to elucidate the mechanism of EMT

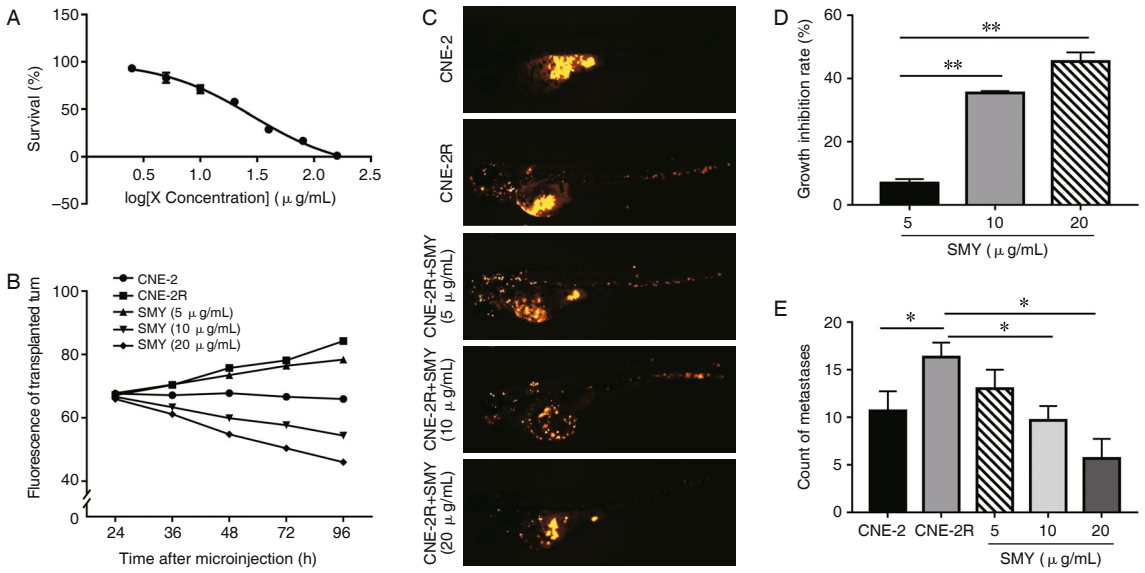

Figure 5. SMY Inhibits Proliferation and Metastasis of CNE-2R Cells in Zebrafish

Notes: (A) Suitable concentration of SMY in zebrafish. (B) The fluorescence intensity of the transplanted tumor decreased after SMY. (C) Fluorescent image of the transplanted model. (D) The growth inhibition rates of the transplanted tumor were calculated as percentages. (E) Comparison of tumor metastasis of zebrafish among groups. SMY: Shengmai Yin. $^{*}P<0.05$, $^{**}P<0.01$

in radiation resistance of NPC cells, text mining and microarray data analysis were further used to identify genes highly related to radiation resistance and EMT of NPC. Although the expression level of LCN2 is low in most human tissues, it is abundant in invasive cancer subtypes. This high level of expression is related to cell proliferation, angiogenesis, invasion, and metastasis.[8] Study has shown that LCN2 participates in the activation of SRC signal transduction and triggers EMT to promote the migration of prostate cancer cells and enhance tumor metastasis.[23] LCN2 can induce vascular endothelial growth factor production, angiogenesis, EMT, and cell migration and invasion through multiple signaling pathways, thereby promoting breast cancer metastasis, including phosphoinositide 3-kinase (PI3K)/protein kinase B (AKT)/nuclear factor kappa B (NF-κB) and hypoxia-inducible factor-1α/Erk.[24] However, the relationship between LCN2, EMT, and radiation resistance in NPC remains unclear. SMY has a radiosensitizing effect in NPC.[15] Using the CCK-8 assay, we found that SMY had an inhibitory effect on CNE-2R cells. After treatment with 100 μg/mL for 48 h, the expression of LCN2 decreased significantly compared to that in the irradiation group. Simultaneously, the expression of Snail, CDH-2, and vimentin also decreased significantly, suggesting that SMY can reverse the EMT process in radiation resistance of NPC through LCN2.

Next, colony formation, wound healing, and invasion assays were conducted. SMY was found to reduce the proliferation, migration, and invasion of CNE-2R cells, indicating that SMY may inhibit the proliferation, migration, and invasion of NPC cells *in vitro* by downregulating the expression of LCN2. Finally, we established a zebrafish xenograft model of CNE-2R cells. By calculating the survival rate and fluorescence changes *in vivo*, we found that SMY could mediate the growth and metastasis of NPC in a dose-dependent manner *in vivo*, which is consistent with the results of *in vitro* studies.

However, our study has some limitations. It will be more convincing to study the mechanism by functionally silencing or knocking out LCN2. Moreover, it is not clear how LCN2 activates signal transduction in NPC cells, and these problems need to be investigated in detail in future studies.

In conclusion, our study provides mechanistic insights into the interaction between radiation resistance of NPC, SMY, LCN2, and EMT, and emphasizes the possible role of SMY in radiation resistance of NPC through LCN2.

Conflict of Interest

The authors declare no conflicts of interest.

Author Contributions

Wang ZT and Peng Y conducted experimental research, collected the test data, elucidated the results. Lou DD

designed this research and wrote the manuscript. Zeng SY and Zhu YC took part in the experiment. Li AW and Lyu Y provided constructive suggestions. Fan Q and Zhu DQ directed the project and managed the funds. All authors read and approved the final version for publication.

Acknowledgement

The authors gratefully acknowledge generous support by of the Radiotherapy Department of Nanfang Hospital.

REFERENCES

1. Lin G, Yu B, Liang Z, Li L, Qu S, Chen K, et al. Silencing of c-jun decreases cell migration, invasion, and EMT in radioresistant human nasopharyngeal carcinoma cell line CNE-2R. Onco Targets Ther 2018;11:3805-3815.
2. Sun Y, Lin H, Qu S, Li L, Chen K, Yu B, et al. Downregulation of CD166 inhibits invasion, migration, and EMT in the radioresistant human nasopharyngeal carcinoma cell line CNE-2R. Cancer Manag Res 2019;11:3593-3602.
3. Yuan X, Zhang L, Huang Y, Liu D, Peng P, Liu S, et al. Induction of interleukin-6 by irradiation and its role in epithelial mesenchymal transition and radioresistance of nasopharyngeal carcinoma cells. Head Neck 2021;43:757-767.
4. Ashrafizadeh M, Zarrabi A, Hushmandi K, Kalantari M, Mohammadinejad R, Javaheri T, et al. Association of the epithelial–mesenchymal transition (EMT) with cisplatin resistance. Int J Mol Sci 2020;21:4002.
5. Zhou D, Ye C, Pan Z, Deng Y. SATB1 knockdown inhibits proliferation and invasion and decreases chemoradiation resistance in nasopharyngeal carcinoma cells by reversing EMT and suppressing MMP-9. Int J Med Sci 2021;18:42-52.
6. Huang Y, Zhang M, Li Y, Luo J, Wang Y, Geng W, et al. miR-183 promotes radioresistance of lung adenocarcinoma H1299 cells via epithelial-mesenchymal transition. Braz J Med Biol Res 2021;54:e9700.
7. Kim SL, Lee ST, Min IS, Park YR, Lee JH, Kim DG, et al. Lipocalin 2 negatively regulates cell proliferation and epithelial to mesenchymal transition through changing metabolic gene expression in colorectal cancer. Cancer Sci 2017;108:2176-2186.
8. Santiago-Sanchez GS, Pita-Grisanti V, Quiones-Diaz B, Gumpper K, Cruz-Monserrate Z, Vivas-Mejía PE. Biological functions and therapeutic potential of lipocalin 2 in cancer. Int J Mol Sci 2020;21:4365.
9. Cheng J, Chen J, Zhao Y, Yang J, Xue K, Wang Z. MicroRNA-761 suppresses remodeling of nasal mucosa and epithelial–mesenchymal transition in mice with chronic rhinosinusitis through LCN2. Stem Cell Res Ther 2020;11:151.
10. An X, Duan LY, Zhang YH, Jin D, Zhao SH, Zhou RR, et al. The three syndromes and six Chinese patent medicine study during the recovery phase of COVID-19. Chin Med 2021;16:44.
11. Li S, Qian Y, Xie R, Li Y, Jia Z, Zhang Z, et al. Exploring the protective effect of ShengMai-Yin and Ganmaidazao decoction combination against type 2 diabetes mellitus with nonalcoholic fatty liver disease by network pharmacology and validation in KKAy mice. J Ethnopharmacol 2019;242:112029.
12. Ming S, Kan M, Liu L, Zhang Z, Liu X, Liu Y, et al. Protective effect of shengmaiyin in myocardial hypertrophy-induced rats: a genomic analysis by 16S rDNA. Evid Based Complement Alternat Med 2022;2022:3188292.
13. Miao M, Li Q, Liu YR. Chemo-sensitivity enhancing effects of Shengmai Injection on various chemotherapeutic drugs. Chinese Traditional and Herbal Drugs 2013;44:875-880.
14. Liu S, Wang Z, Zhu D, Yang J, Lou D, Gao R, et al. Effect of Shengmai Yin on the DNA methylation status of nasopharyngeal carcinoma cell and its radioresistant strains. J Pharm Anal 2021;11:783-790.
15. Liu S, Wang Z, Zhu D, Yang J, Lou D, Gao R, et al. Effect of Shengmai Yin on the DNA methylation status of nasopharyngeal carcinoma cell and its radioresistant strains. J Pharm Anal 2021;11:783-790.
16. Zhu D, Huang M, Fang M, Li A, Liu Z, Shao M, et al. Induction of radioresistant nasopharyngeal carcinoma cell line CNE-2R by repeated high-dose X-ray irradiation. Int J Radiat Res 2019;17:47-55.
17. Tsering J, Hu X. Triphala suppresses growth and migration of human gastric carcinoma cells *in vitro* and in a zebrafish xenograft model. Biomed Res Int 2018;2018:7046927.
18. Wu JQ, Zhai J, Li CY, Tan AM, Wei P, Shen LZ, et al. Patient-derived xenograft in zebrafish embryos: a new platform for translational research in gastric cancer. J Exp Clin Cancer Res 2017;36:160.
19. Chen YP, Chan A, Le QT, Blanchard P, Sun Y, Ma J. Nasopharyngeal carcinoma. Lancet 2019:394:64-80.
20. Sun XS, Li XY, Chen QY, Tang LQ, Mai HQ. Future of radiotherapy in nasopharyngeal carcinoma. Br J Rad 2020;92:20190209.
21. Zackrisson B, Mercke C, Strander H, Wennerberg J, Cavallin-Ståhl E. A systematic overview of radiation therapy effects in head and neck cancer. Acta Oncol 2003;42:443-461.
22. Suna ZMZ, Chao Z, WANG W, Haihua Y, Wenguang YE. The role of epithelial-mesenchymal transition in regulating radioresistance. Crit Rev Oncol Hematol 2020;150:102961.
23. Lu Y, Dong B, Xu F, Xu Y, Pan J, Song J, et al. CXCL1-LCN2 paracrine axis promotes progression of prostate cancer via the Src activation and epithelial-mesenchymal transition. Cell Commun Signal 2019;17:118.
24. Hu C, Yang K, Li M, Huang W, Zhang F, Wang H. Lipocalin 2: a potential therapeutic target for breast cancer metastasis. Onco Targets Ther 2018;11:8099-8106.

(Accepted July 18, 2022; First Online December 7, 2022)
Edited by YUAN Lin